

Development of a 4K Pulse-Tube Cold Finger for Space Applications

A. Charrier¹, I. Charles¹, B. Rousset¹, C. Daniel² and J.-M. Duval¹

¹ Univ. Grenoble Alpes, CEA INAC-SBT, Grenoble, France

² CNES Centre National d'Etudes Spatiales, Toulouse, F-31401, France

ABSTRACT

A sub-Kelvin cryogenic cooling chain without a helium bath is a challenge for space missions. A 4.2K pulse-tube cryocooler working at high frequency (around 30Hz) is one option to meet the challenge.

A low temperature pulse tube can be integrated into the next astrophysics space missions like ATHENA + (Advanced Telescope for High ENergy Astrophysics), PRISM (Polarized Radiation Imaging and Spectroscopy Mission) or TALC (Thin Annular Light Collector) that require sub-Kelvin temperatures for ultra-sensitive detectors. Several tens of mW in the 4K-5K temperature range is the order of magnitude for the cooling power requirement.

The apparatus studied is composed of two compressors (one main and one active phase shifter) and a pulse-tube cold finger with two regenerators separated by an intercept (heat exchanger) cooled by a Gifford-McMahon cryocooler.

This work has focused on the cold part of the cold finger. The impact of the specific heat of the porous media used in the cold regenerator has been studied. Experimental results, such as load curves, cold end temperature fluctuations, impact of the power of the main compressor, are presented and analyzed. This pulse tube has been tested and optimized and temperatures below 4K have been obtained with a frequency of 30Hz and an intercept temperature of 20K.

INTRODUCTION

Cooling power at low temperature is necessary for astrophysics space missions where the sensors have to be cooled to be able to work efficiently.

The CEA-SBT is developing efficient cryocoolers for earth observation or for a wide variety of missions dedicated to the understanding of the universe. A part of its work is focused on the pulse tube, especially on the high frequency (around 30Hz) devices. For example, a 15K pulse-tube cooler has been developed with Air Liquide and Thales Cryogenics B.V. within the framework of a Core Technology Program funded by ESA to address the needs of Athena [1].

The next step is the 15K-4K range where helium does not act like a perfect gas. It has been studied by several teams including a Chinese one [2] and an American one [3] in the last few years and interesting performance results have been reported.

This paper focuses on the 4K temperature range. A prototype has been optimized for operations at lower temperatures and is being improved.

EXPERIMENTAL SETUP

Cold finger design

The pulse tube has a coaxial configuration with two regenerators (crosshatch in Figure 1), one warm and one cold, separated by an intercept. This intercept is a heat exchanger (dots in Figure 1) in copper which is linked to a Gifford-McMahon (GM) cryocooler to precool the cold part of the cold finger.

The warm regenerator is filled with stainless steel meshes. The cold regenerator is filled with rare earth regenerator materials developed at CEA. The temperature of the intercept is regulated with a heater. The pulse-tube cold finger uses an active phase shifter (for more details see [4]).

Configurations and porous materials with specific heat anomalies

Several different configurations have been tested. The guiding thread is the specific heat capacity of the porous media included in the cold regenerator.

Four configurations, as seen in Figure 2, have been tested with different grading. In all of the configurations, the “shape” of the regenerator and the hydraulic parameters (porosity, friction factor) have been kept constant. Only the specific heat has been changed for the results presented in this paper. Three different materials have been used as part of this work and will be called “R compound” (R for reference), “A compound” and “B compound” in this paper.

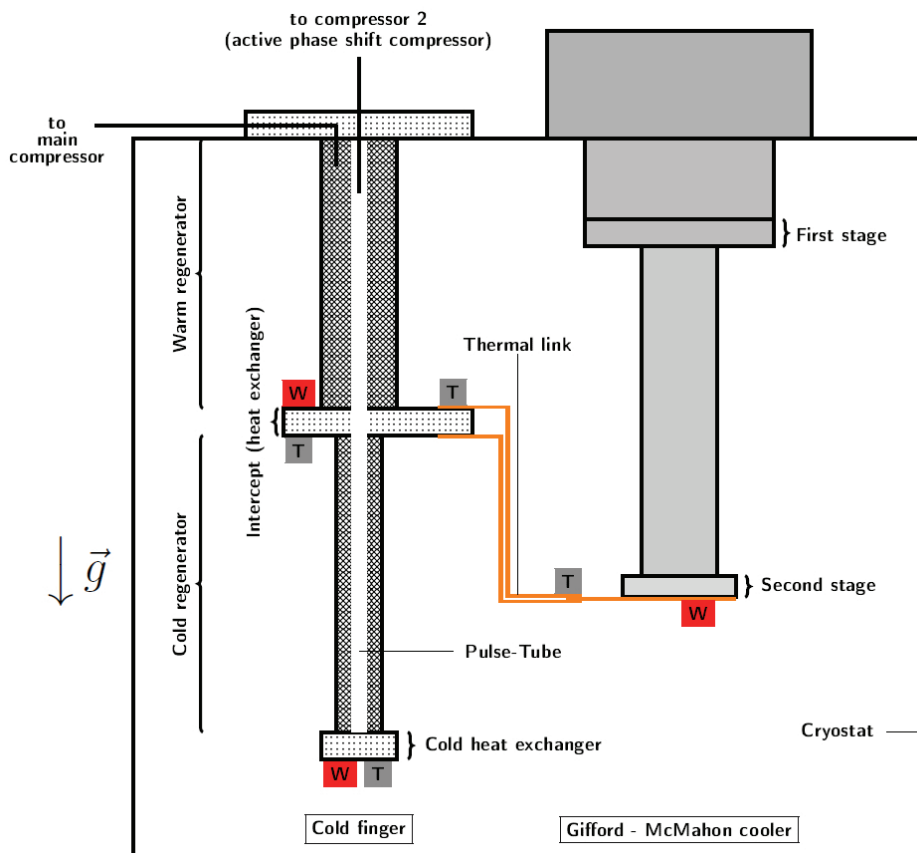


Figure 1. Schematic view of the cold finger linked with the Gifford-McMahon

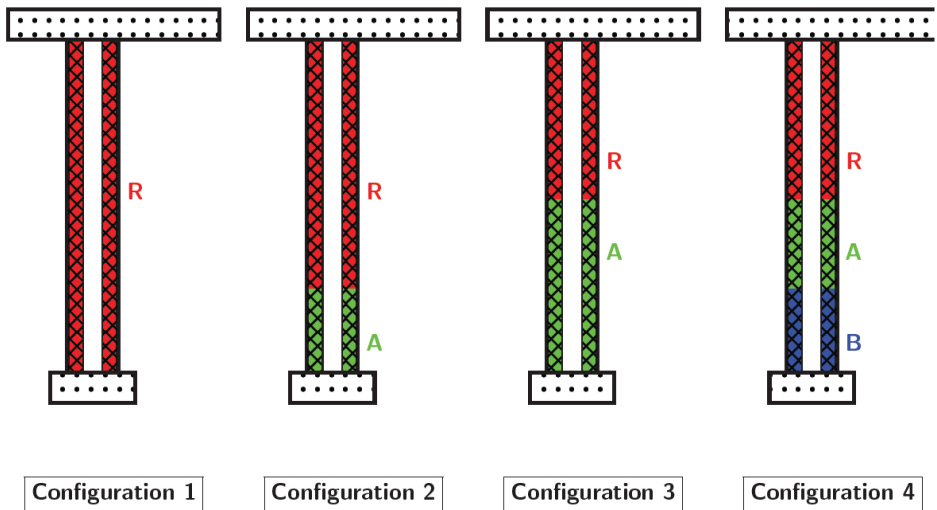


Figure 2. The four configurations tested (the intercept is at the top and the cold end at the bottom)

The choice of the porous media put in the cold regenerator was based on knowing the specific heat capacity of the elements (see Figure 3).

- The specific heat capacity of the reference compound is slowly decreasing with decreasing temperature without any anomaly.
- The specific heat capacity of the A compound presents a wide anomaly around 10K-14K up to 1.2 times higher than the reference in this range.
- The specific heat capacity of the B compound presents a wide anomaly around 5K-10K up to 2.6 times higher than compound A in this temperature range.

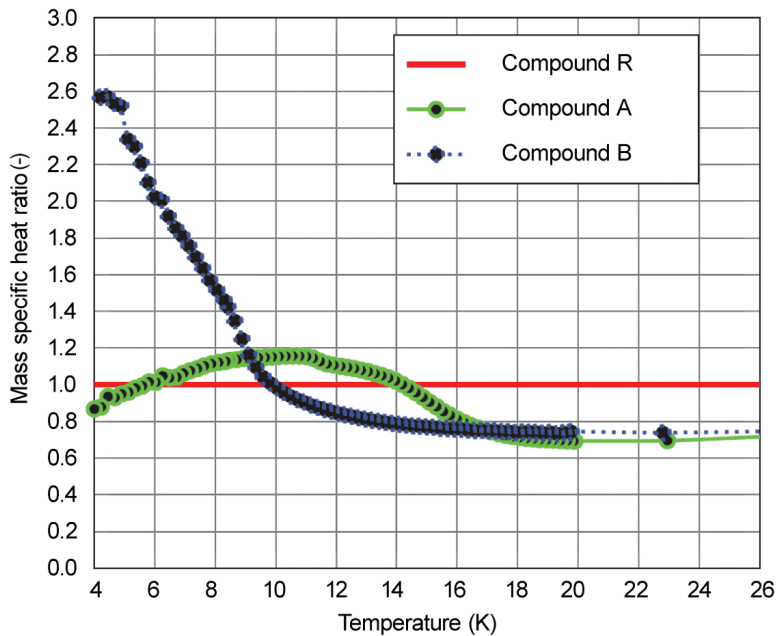


Figure 3. Mass specific heat ratio of the three compounds

EXPERIMENTAL RESULTS AND ANALYSIS

Performances at 100 W PV

For all of the configurations and cooling powers tested, the active phase shift was optimized to obtain the best performances except for the ultimate temperature due to compressor stroke limitation (see Figure 4). To complete the curve of the fourth configuration, the no-load temperature was plotted for 87.5 W_{PV} (the value at 100W_{PV} was not available when the paper has been written).

The measurement uncertainty of the thermometer and readout varies with the temperature range. The Cernox thermometer has a maximum uncertainty of 0.02K over the 4K-20K range.

Figure 5 shows the performance obtained with the different configurations tested.

Including a material with a higher specific heat than the reference in the lowest part of the regenerator increases the performance. The gain is 70mW around 9K between the first, the second and the third configuration.

In Configuration 3, the quantity (the length) of material with a higher specific heat was increased up to 60% of the regenerator length compared to Configuration 2. Below a 10K cold end temperature, Configuration 2 and 3 are quite similar (the specific heat anomaly of the A compound is in the appropriate location to be used in both configurations) but when the cold end temperature is above 10K-11K, one part of the A compound is in a temperature range where its specific heat capacity is lower than the one of the reference material and as a consequence the performance of the third configuration is worse than those of the Configuration 2.

The fourth configuration, partially tested (test in progress) is the best to achieve low temperatures: two different compounds with specific heat anomalies at different temperature ranges have been used to create a porous media allowing continuous high specific heat along the cold regenerator. The graph highlights that 50mW of cooling power is available at 5.97K.

Mechanical power of the main compressor and swept volume: limitation of the ultimate temperature at high PV

The mechanical power (PV power) of the main compressor impacts the performance of the cold finger, as shown in Figure 4, but is limited by the swept volume of the main compressor.

The swept volume of the main compressor varies with the temperature of the cold end and has an inflection point (around 9K) in the area where the property of helium changes sharply.

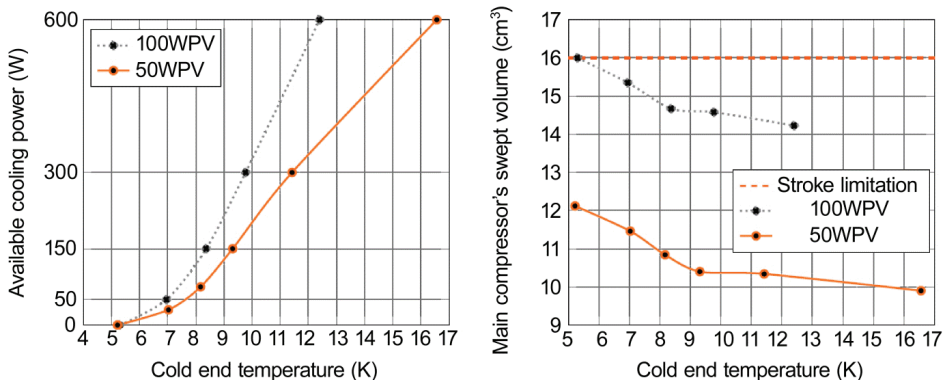


Figure 4. Impact of the power of the main compressor on the performances and on the swept volume (Configuration 2).

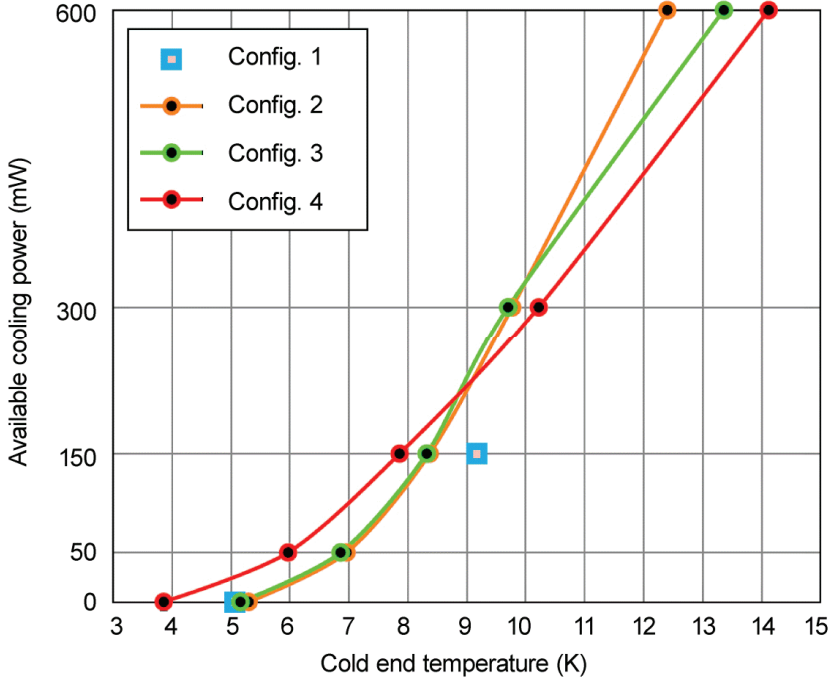


Figure 5. Load curves at 100W_{PV} and 20K intercept

The density is probably an important factor in this behavior: the helium’s density is rising over the complete temperature range. A larger swept volume is needed to completely fill the cold finger at low temperature.

The cold end temperature is reduced when the input power is increased from 50W_{PV} to 100W_{PV}, for each point of the load curve except for the no-load temperature because of the swept volume limitation at 100WPV (studies have to be done at a lower WPV to overcome the stroke limitation and to reach a lower no-load temperature).

Lowest temperatures obtained (75W_{PV} and 87.5W_{PV} / 0mW cold end)

As previously mentioned, the limitation of the swept volume of the main compressor was an issue for obtaining the lowest temperature at 100W_{PV}. Some measurements have also been performed at 75W_{PV} and at 87.5W_{PV} for the key configurations (see Table 1).

The heat rejected at the intercept for the lowest point (3.86K) is around 8.6W but this value could be decreased by adding another thermal link at the warm regenerator [1].

As shown previously [4], the higher mechanical power provided to the gas results, the lower ultimate temperature becomes. Therefore, we can assume that a lower temperature could have been obtained if a bigger compressor would have been available.

Table 1. Best performances obtained

	Configuration 3	Configuration 4	
Power	75W _{PV}	75W _{PV}	87.5W _{PV}
Cold end temperature	4.90K	3.92K	3.86K

Impact of the temperature of the intercept (20K and 50K)

The impact of the intercept temperature has also been studied. The choice, the location and the quantity of the different porous media placed in the cold regenerator have been studied for efficiency when the intercept is maintained at 20K and for a low temperature of 5K. The degradation of the performance due to a change in the intercept temperature can be seen in the Table 2. Raising the intercept temperature from 20K to 50K leads to a degradation of performance, which increases when the temperature of the cold end rises. This degradation can be associated with the use, or not, of the local high specific heat of the compounds in the appropriate temperature range.

PARASITIC LOSSES

Description of the system

The parasitic losses corresponding to the heat load when the cooler is OFF have been studied. The cryostat has been turned upside down (cf. Figure 6): the cold end is now at the top and the hot heat exchanger is now at the bottom. The system has been purged of its helium (to limit convection heat transfer). The temperature of the intercept is maintained at 11K thanks to the GM cryocooler. Different powers are dissipated at the cold end of the cold finger.

Results

The procedure induces a thermal gradient in the second regenerator which is in the opposite direction from the one of the actual experiment. For this reason, the only configuration which can properly be analyzed is the first configuration where the regenerator is homogenous. Moreover the impact of helium on the results is not studied (system purged to avoid convection in the central tube) and the cold end temperature simulated here by the heat intercept cannot be cooled lower than 11K (limitation to go lower due to the GM and thermal link performances).

Parasitic losses in pulse tube have been studied in the past on stacked screens and porous media [5] [6]. The conduction through the porous media is a non-negligible problem for the cryocooler's performance. In fact, it has been reported that the conduction losses are equivalent to a conduction through around 10% of the cross section S occupied by the regenerator matrix ($S = \text{regenerator cross section} * (1 - \text{porosity})$) [5] [6].

A similar analysis has been performed on our system with a specific test campaign. After treatment, to fit the experimental curve, a contribution of around 30% of cross section S occupied by the porous media had to be taken into account if we consider a porous media having the thermal conductivity of stainless steel (cf. Figure 7).

Without power dissipated at the cold end, a temperature difference between the intercept and the cold end is already observed. This difference implies an initial parasitic load which is around 4mW probably due to internal radiation from ambient temperature (and some remaining convection).

Table 2. Impact of the temperature of the intercept on the performances of the cold finger

	$T_{\text{intercept}} = 20\text{K}$		$T_{\text{intercept}} = 50\text{K}$	
	50mW	600mW	50mW	600mW
Configuration 2	6.96K	12.40K	7.27K	14.21K
Configuration 3	6.86K	13.36K	7.17K	15.44K

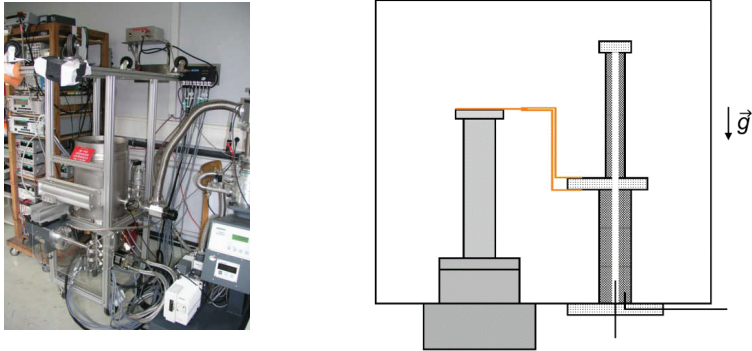


Figure 6. System to study the parasitic losses (photo and schematic)

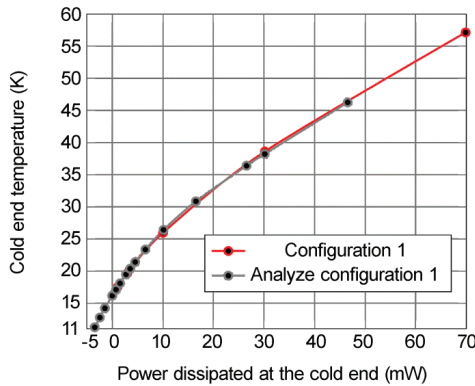


Figure 7. Parasitic losses of the system under the first configuration

Using the correlation found for the parasitic heat losses above 11K, the contribution for the case with an intercept at 20K and a cold end at 5K due to walls and porous media conduction leads to a thermal loss of around 9mW. The total load reaching the cold end at 5K with an intercept at 20K is around 13mW (see Table 3).

This could be translated into a cold end temperature rise of around 0.4K (value obtained from the load curve), which is not negligible. Nevertheless, the temperature rise is probably overestimated due to the fact that the actual thermal gradient in the regenerator at the cold end is not the same for an operating cooler as it would be for an OFF cooler. The thermal gradient at the cold end is smaller for an operating cooler than for an OFF cooler. It should be noted that the conduction through the porous media is responsible for half of the estimation of parasitic losses.

Table 3. Parasitic loads on Configuration 1

		Parasitic load (mW)	Estimation of temperature rise (K)
Initial	Radiation, convection	4	0.13
Gradient between 5K and 20K	Conduction through the walls	3	0.10
	Conduction through the porous media	6	0.20
Total	Radiation, conduction, convection	13	0.43

SHAPE OF THE LOAD CURVES

It could be surprising that the shape of the cooling curve suggests that it becomes easier to produce cooling power when the temperature is lower than 10K (inflexion point around 10K). In Figure 5, unlike the usually observed behavior, the derivative of the cooling power increases with temperature (curved to the top).

One explanation could be that the helium no longer acts like a perfect gas in this temperature range. A calculation has been done using data from a classic case: knowing the average pressure on the system (20bars), and the delta of pressure in the tube (3bars), the high pressure and the low pressure of the system are deduced. The entropy is calculated using HePak and knowing the high pressure value and the high pressure temperature value. If the expansion in the tube is considered to be isentropic, the low pressure temperature can be calculated with the entropy and the low pressure. The high pressure and low pressure enthalpies are calculated and the difference of these two enthalpies gives the ΔH plotted on the graph below.

The isentropic expansion assumption can also be applied to a perfect gas. Knowing the high pressure, the low pressure and the high pressure temperature, the low pressure temperature is obtained from the $T^\gamma P^{1-\gamma} = \text{constant}$ equation and then $\Delta H = C_p \Delta T$.

It is not surprising that helium gas behaves roughly as a perfect gas at high temperature. At low temperature, the linear trend (Figure 8 left) gives way to a curved line which resembles the shape of the load curves that have been measured previously.

It can clearly be seen in Figure 8 (right) that there is a change of trend at 10K and that the real gas starts to become better (ratio > 1) at lower temperature compared to the perfect gas.

COLD END TEMPERATURE FLUCTUATION

One way of verifying if the isentropic expansion assumption is a good approximation consists of measuring both the temperature and the pressure fluctuations and correlating the results with an isentropic behavior. To do so, a Cernox thermometer located on the cold heat exchanger is used. The system is also equipped with several sensors measuring transient pressure with one located on the main compressor in the compression chamber measuring the “steady state” pressure only. The pressure sensor located at the exit of the cold finger allows the measurement of the peak-to-peak value of the pressure wave.

This value allows the determination of the high pressure and the low pressure at the cold end and the correlation with the cold end temperature fluctuations (see Figure 9 right) measured by a fast acquisition system connected to a Cernox thermometer [4]. The response time of the temperature sensor is an important unknown.

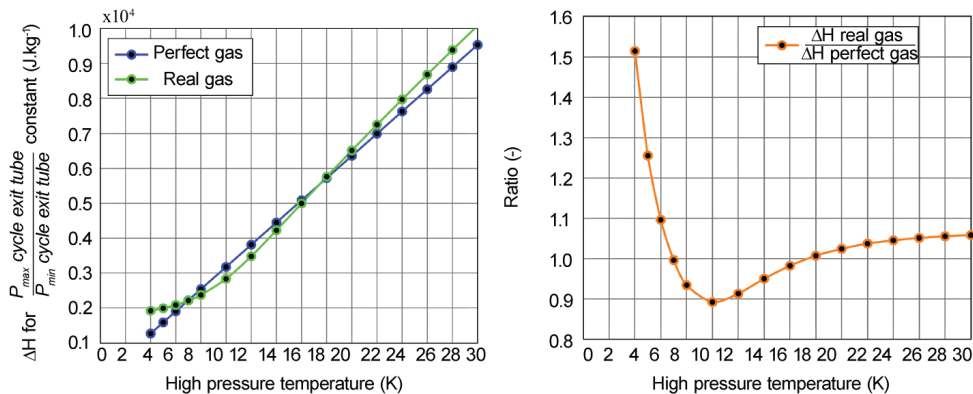


Figure 8. Evolution of the enthalpy difference of the gas due to an isentropic expansion at different cold end temperature (left) and ratio of the enthalpy difference for real and perfect gas (right).

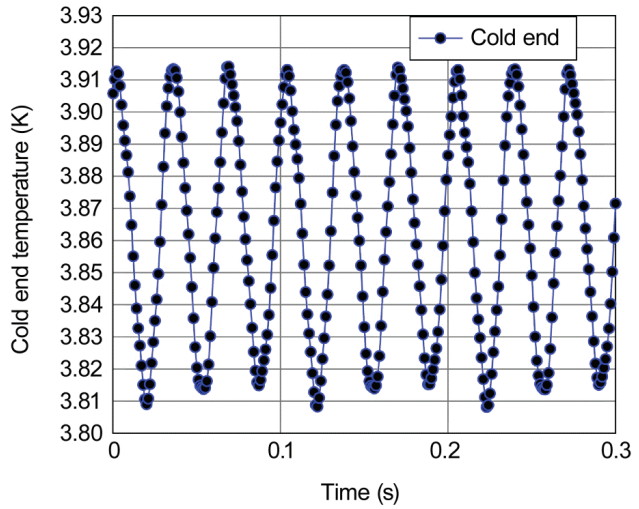


Figure 9. Cold end thermometers [Cernox thermometer and platinum sensor] and heater (left) and Cold end temperature fluctuations [average P = 17.45 bars and ΔP tube exit = 4.03 bars] (right)

An analogy can be done between a RC circuit and the system under study: the R part is a global heat transfer coefficient between the gas and the sensible part of the thermometer (three resistances exist: one between the gas and the exchanger, one between the exchanger and the packaging of the thermometer and, finally, one between the packaging of the thermometer and the sensible part of the thermometer) and the C part is a global thermal capacity of the global system (exchanger, thermometer packaging and sensible part of the thermometer).

In the following, the assumption that this system can be represented by a first order RC system has been made. An experimental case has been studied and the temperature fluctuations of the cold end temperature have been compared with what can be expected in the ideal case of an isentropic expansion. The measured temperature is very close to the theoretical value obtained for an isentropic expansion. This allows for determining a conservative value for the damping (13%) that could be due to thermometer sensor time response. From this damping measured at 30Hz and assuming a first order RC system, the time response of the thermometer sensor is better than 3ms, much better than the information given by LakeShore (see Table 4).

CONCLUSION

A coaxial pulse tube has been designed which features a heat intercept. This heat intercept has been precooled by a GM cooler to study the impact of the specific heat of the porous media in the cold regenerator. Different regenerator materials with specific heat anomalies have been tested using different regenerator grading. A temperature as low as 3.86K was obtained with an

Table 4. Summary of the parameters used to estimate the time response

High pressure	19.465 bars
Low pressure	15.435 bars
Frequency	30Hz
ΔT experimental	0.11K
ΔT theoretical (assuming isentropic expansion)	0.13K
Damping	13%
Time constant RC circuit	3ms
Supplier (Lakeshore) response time	Between 15ms and 400ms at 4.2K

intercept temperature maintained at 20K. With the best configuration presented in this paper, a cooling power of 50mW is available at 5.97K. The test campaign has been done using helium-4. Better performances should be obtained with the same configuration using helium-3. With a linear extrapolation of the experimental data at $100W_{PV}$, around 15mW should be available at 4.5K which is close to the cooling power produced by the Joule-Thomson cryocooler that flew on the Planck mission. These improvements represent a milestone in the development of a cryogenic system without a helium bath.

ACKNOWLEDGMENT

The project is supported by the Atomic Energy Commission (CEA) and by the French National Space Agency (CNES). The authors acknowledge Gérard LAPERTOT (SPSMS), Stéphanie POUGET (SGX) and Christophe MARIN (SPSMS) for contributions to material developments and constructive discussions. The authors acknowledge Alexandre COYNEL (SBT) for his technical support during all the experiments. The authors acknowledge Anthony ATTARD (SBT), Daniel COMMUNAL (SBT) and Thierry JOURDAN (SBT) for the development of high frequency temperature readout.

REFERENCES

1. Duval, J.M., Charles, I., Butterworth, J., Mullie, J. and Linder, M., "7K-15K Pulse-Tube Cooler for Space," *Cryocoolers 17*, ICC Press, Boulder, CO (2013), pp. 17-23.
2. Zhi, X.Q., Han, L., Dietrich, M., Gan, Z.H., Qiu, L.M. and Thummes, G., "A three stage stirling pulse tube cryocooler reached 4.26K with He-4 working fluid," *Cryogenics*, Vol. 58 (2013), pp. 93-96.
3. Nast, T., Olson, J., Champagne, P., Mix, J., Eytimov, B., Roth, E. and Collaco, A., "Development of a 4.5K Pulse Tube Cryocooler for Superconducting Electronics," *Adv. in Cryogenic Engineering*, Vol. 53, Amer. Institute of Physics, Melville, NY (2008), pp. 881-886.
4. Charrier, A., Charles, I., Rousset, B., Duval J.-M. and Daniel, C., "Low temperature high frequency coaxial pulse tube for space application," *Adv. in Cryogenic Engineering*, Vol. 59, Amer. Institute of Physics, Melville, NY (2014), pp. 1010-1017.
5. Lewis, M.A., Kuriyama, T., Kuriyama, F. and Radebaugh, R., "Measurement of heat conduction through stacked screens," *Adv. in Cryogenic Engineering*, Vol. 43, Amer. Institute of Physics, Melville, NY (1998), pp. 1611-1618.
6. Lewis, M.A. and Radebaugh, R., "Measurement of Heat Conduction through Bonded Regenerator Matrix Materials," *Cryocoolers 12*, Kluwer Academic/Plenum Publishers, New York (2003), pp. 517-522.